Water Level Observations and Short-Term Predictions Including Meteorological Events for Entrance of Galveston Bay, Texas

Daniel T. Cox, M.ASCE[1]; Philippe Tissot[2]; and Patrick Michaud[3]

Abstract: This paper shows that conventional harmonic analysis alone does not adequately predict the coastal water level variation at the entrance to Galveston Bay when strong meteorological forcing is present. The water level anomalies (the difference between the observed water level and that predicted by harmonic analysis) are shown to be as large as the tidal range itself. The water level anomaly at the entrance to Galveston Bay is primarily due to the east-west directed wind speed, and a simple linear model is shown to predict the anomaly based on the locally measured wind and a nine hour lag between the wind forcing and water level response. The model is further refined using a neural network approach with east-west and north-south winds, barometric pressure, and the previously observed water level anomaly and without assuming previous knowledge of the phase lag between wind and water level. Both linear and neural network models are shown to improve significantly short-term ($3<t<24$ h) predictions of the total water level using forecasted wind speed and direction.

DOI: 10.1061/(ASCE)0733-950X(2002)128:1(21)

CE Database keywords: Water levels; Texas; Tides; Storm surges; Neural networks; Prediction.

Introduction

The coastal waters of the northern Gulf of Mexico are characterized by one of the longest estuarine environments in the world. These waterways play a critical economic role and affect shipping, oil and natural gas production, recreation, tourism, fisheries, and environmental habitat. Understanding tidal and subtidal water level fluctuation and circulation along the coast is important for safe navigation, water quality, and emergency management such as oil spill response, search and rescue operations, and evacuation during extreme weather events.

The need for reliable water level forecasting is increasing with the trend toward deep-draft vessels, particularly for shallow water ports along the Gulf of Mexico (NOAA 1999). Nine of the 12 largest U.S. ports with tonnage greater than 50 million tons are located along the Gulf of Mexico, accounting for 52.3% of the U.S. total tonnage (NOAA 1999). Ports served by the Mobile Bay Entrance and Galveston Bay Entrance alone account for 46% of the total U.S. tonnage. Although the astronomical tides in the Gulf of Mexico are easily predicted by conventional harmonic analysis, it is difficult to accurately predict the total water level fluctuations because of frequent meteorological events, such as the passage of strong cold fronts. For example, the Corpus Christi, TX, airport is ranked by the National Weather Service as the third windiest in the U.S. based on a multiannual average wind speed of 23.5 kph (Smith 1978). In a report focusing on harmonic predictions of water levels and currents in Corpus Christi, NOAA (1994) indicated that existing tidal current tables were outside of established National Ocean Service (NOS) working standards. New predictions derived from standard harmonic analysis showed only a ''slight improvement,'' and the report cited the lack of including meteorological conditions as the primary factor accounting for discrepancies between observed and predicted currents and water levels. The report concluded that future efforts should address the relationship between wind direction and ''exaggerated tidal currents and water level fluctuations.''

Our inability to accurately predict water level fluctuations can have severe consequences, such as ship groundings. To better improve navigation and safety in these waterways, NOAA has established the Physical Oceanographic Real-Time System (PORTS), which includes the near real-time monitoring and reporting of water levels and meteorological conditions via telephone or Internet (http://www.co-ops.nos.noaa.gov/). Although this system has greatly decreased navigational hazards along the northern Gulf of Mexico coast, PORTS relies on harmonic analysis for water level predictions and presently does not incorporate meteorological information into the forecasts. The purposes of this paper are: (1) to show the limitations of the water level predictions for the entrance to Galveston Bay using harmonic analysis alone; (2) to suggest an improved method whereby the water level anomaly (difference of measured water level and predicted tide level) can be predicted using the observed local wind speed; and (3) to refine this model using a neural network approach.

Observations

The observations for this paper were taken on the open coast near the entrance to Galveston Bay on Pleasure Pier, Galveston Island,

[1]Coastal and Ocean Engineering Division, Dept. of Civil Engineering, Texas A&M Univ., College Station, TX 77843.

[2]Conrad Blucher Institute for Surveying and Science, Texas A&M Univ.-Corpus Christi, Corpus Christi, TX 78412.

[3]Conrad Blucher Institute for Surveying and Science, Texas A&M Univ.-Corpus Christi, Corpus Christi, TX 78412.

Note. Discussion open until June 1, 2002. Separate discussions must be submitted for individual papers. To extend the closing date by one month, a written request must be filed with the ASCE Managing Editor. The manuscript for this paper was submitted for review and possible publication on February 16, 2001; approved on June 15, 2001. This paper is part of the ***Journal of Waterway, Port, Coastal, and Ocean Engineering***, Vol. 128, No. 1, January 1, 2002. ©ASCE, ISSN 0733-950X/2002/1-21–29/$8.00+$.50 per page.

Fig. 1. Overview of TCOON stations and study area at Pleasure Pier

TX, as shown in Fig. 1. The hydro-meteorological station is operated by the National Ocean Service as part of its National Water Level Observation Network. The data for this station are provided by the Conrad Blucher Institute for Surveying and Science at Texas A&M University–Corpus Christi as part of the Texas Coastal Ocean Observation Network (TCOON) (Michaud et al.1994). TCOON consists of over 40 stations with real-time access made available through Internet and other media. All stations report water level, and many others (including the Pleasure Pier station used in this study) report wind speed, direction, gust, air temperature, water temperature, and barometric pressure. TCOON has been in operation for over ten years, and three TCOON stations provide data to the PORTS system.

For this paper, representative data were taken from the Pleasure Pier station for two seasons in the spring (A) and summer (B) months over three years from 1997 to 1999. The statistics characterizing these observations are listed in Table 1. The 1998 time series of observed and predicted water level is shown in Fig. 2 with the details from Season A and B. Season A ran from approximately January to April and was characterized by strong frontal systems that passed over the region. Season B ran from approximately June through July and was characterized by an almost flat barometric pressure reading over the period and winds primarily due to local thermal effects (sea breeze). Fig. 2 also shows two large water level anomalies between $230<Jd<260$ corresponding to tropical storms Charley and Frances, which made landfall on the Texas coast. Events such as these and their associated storm surges are not considered in this paper. Our focus, instead, is on the water level anomaly due to frontal systems that occur with greater frequency. The water level anomaly associated with the passage of these fronts can be as large as the tidal variation itself (see Fig. 2; $Jd \simeq 67$).

Table 1 lists the years of the observation (column 1); the range of days considered (Jd = Julian Day) (2); the number of days in the record N_{day} (3); the maximum of the absolute observed water level $|H|_{\max}$ (4); the mean wind speed WS (6); the mean barometric pressure P (8); the mean atmospheric temperature T_A (10); and the mean sea temperature T_S (12). The standard deviation σ for these quantities are also listed. All observations were recorded at hourly intervals. Of the statistics listed in Table 1, the most telling is the standard deviation of the barometric pressure, σ_P, which is about three times larger for Season A than for Season B. The large variations in P for Season A give rise to winds that shift rapidly in direction with the passage of the fronts. This significantly influences the water level anomaly and is studied in detail in the next section.

Tide Prediction and Water Level Anomaly

The limitations of water level predictions based on the harmonic analysis are assessed for Galveston for the two seasons listed in Table 1. The average error E for the prediction methods is defined as

$$E = \frac{\left[\frac{1}{N}\Sigma_{i=1}^{N}(H-X)^2\right]^{1/2}}{H_{\text{rms}}} \tag{1}$$

where H = observed water level; H_{rms} = root-mean-square of the observed water level; X = water level prediction based on harmonic analysis; and N = number of observations, $N = 24N_{\text{day}}$. Using this estimate, the average error for the two seasons is $E = 0.78$ and 0.65 for Seasons A and B, respectively.

Although inspection of Fig. 2 would suggest that the error for Season B should be much lower, the relatively large error here is due to the offset between observations and predictions caused by long-term climatic effects. Under these conditions, the simplest method to improve the water level prediction would be to use the known anomaly at the present time t and add that to the prediction at a time $t+j$ hours, where j is the length forecasted time. This is termed the ''adjusted method'' and the resulting prediction is the ''adjusted water level.''

Fig. 3 shows the applicability of this approach for Seasons A and B. In the figure, the average error for the unadjusted water level ($E = 0.78$ and 0.65) is shown by the horizontal dashed line. The error of the adjusted water level is shown by the discrete points for the individual years listed in Table 1, and the average of those points is shown by the solid line. For Season A, the error

Table 1. Statistics of Hydro-Meteorological Observations for Galveston Pleasure Pier

Observation period			$\lvert H\rvert_{\max}$	σ_H	$\overline{WS}$	σ_{WS}	$\overline{P}$	σ_P	$\overline{T_A}$	σ_{T_A}	$\overline{T_S}$	σ_{T_S}
Year	Julian Day	N_{day}	(m)	(m)	(m/s)	(m/s)	(kPa)	(kPa)	(°C)	(°C)	(°C)	(°C)
1999a	$10<Jd<100$	90	0.94	0.23	5.2	2.5	101.63	0.57	17.4	3.3	—	—
1998a	$30<Jd<120$	90	1.03	0.25	5.5	2.5	101.30	0.65	16.8	3.7	17.8	2.8
1997a	$30<Jd<120$	90	0.81	0.24	5.9	2.7	101.58	0.67	16.6	3.9	17.3	3.1
1999b	$185<Jd<225$	40	0.66	0.21	4.5	2.2	101.55	0.25	28.9	1.2	30.3	0.8
1998b	$180<Jd<220$	40	0.67	0.20	5.7	2.2	101.49	0.21	29.2	0.8	30.5	1.0
1997b	$220<Jd<250$	30	0.54	0.19	5.0	2.2	101.51	0.23	29.1	1.1	30.6	0.8

J. Waterway, Port, Coastal, Ocean Eng., 2002, 128(1): 21-29

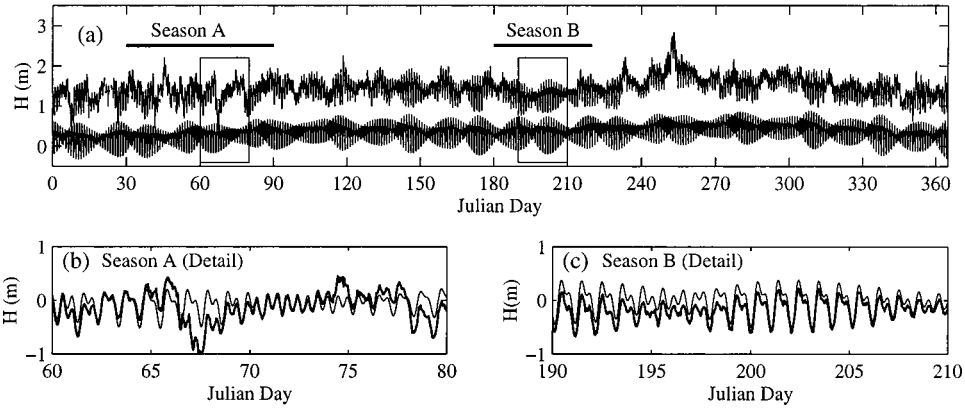

Fig. 2. Comparison of observed and predicted water level for Galveston Pleasure Pier, 1998: (a) Observed record (upper curve offset by 1.4 m for clarity) and tide prediction by harmonic analysis (lower curve). Horizontal lines indicate extent of Season A and B. Detail of Season A (b) and detail of Season B (c) where water level observations are indicated by heavy line and tide predictions by light line.

increases approximately linearly as the extent of the forecast increases from $t=0$ (no error) to a maximum after two days where the error exceeds that of the unadjusted water level. In other words, only very short-term water level predictions, $0<t<3$ h, would benefit from this simple method during Season A. This is because the water level anomaly can change sign within a matter of hours of the passage of a cold front, as shown in Fig. 2. For Season B, however, the error increases more slowly, because the anomaly is generally caused by phenomena acting on a longer time scale such as evaporation, gradual increases in water temperature (e.g., Whitaker 1971), or currents on the continental shelf (e.g., Cochrane and Kelly 1986). The remainder of the paper emphasizes improvements to the short-term water level predictions for Season A with forecasts in the range of $3<j<30$ hours, since this is the time scale of concern for navigation, oil spill response, and search and rescue operations.

To develop a model that will account for the meteorological effects, it is necessary to study the basic relation between wind (forcing) and anomaly (response). Fig. 4 shows a typical variation of water level, air temperature, wind speed and direction, and barometric pressure at Galveston Pleasure Pier for $60<Jd<85$, 1999. The difference, as shown in Fig. 4(a), between the observed water level (shown by the heavy solid line) and the prediction (light line) is the anomaly, as given in Fig. 4(e). The passage of a cold front can be seen for $72<Jd<73$. Prior to the front, the air temperature was warm and winds were out of the east and southeast. This gave rise to a large positive anomaly as water was forced onto the coast by wind setup and wind driven current. With the passage of the front, the temperature dropped rapidly, the winds shifted to be out of the northwest, and the sign of the anomaly changed from positive to negative. The peak negative anomaly was as large as the astronomical tide. Although there are other causes of the water level anomaly, such as the change in the barometric pressure, rainfall, evaporative effects, and air/sea temperature differences, the wind speed and direction are assumed to be the primary forcing mechanisms (e.g., NOAA 1994). The annual variation of the sea level due to steric effects at Galveston is on the order of 10 cm (Whitaker 1971).

To better assess the relationship between the wind and water level anomaly in Galveston, the anomaly is plotted as a function of wind speed square, since it is proportional to the wind stress (e.g., Wu 1980) and direction. Fig. 5 shows the anomaly in polar coordinates. The magnitude of the anomaly is indicated by the symbol where the range for each symbol is normalized by the standard deviation of the tidal signal over that period, σ_X. These values were essentially the same for Season A for each of the three years ($\sigma_X=0.198$, 0.195, and 0.192 m for 1999, 1998, and 1997). These figures show that the largest negative anomalies ($H-X<-3\sigma_X$) are generally associated with wind from the west ($\theta=270$) and the positive anomalies ($H-X>3\sigma_X$) are associated with wind from the east ($\theta=90$). Weak anomalies ($-\sigma_X<H-X<\sigma_X$) follow a similar trend but are not shown for clarity. The average anomaly data from Season A for the three years, including the weak anomalies, are shown in Fig. 6. The size of the data point gives a qualitative indication of the magnitude of the anomaly plotted at that location. The exact magnitude is listed in Table 2, along with the mean of the wind speed squared and direction.

Linear Model

Fig. 6 and Table 2 indicate how both wind speed and direction play an important role in determining the anomaly and that the

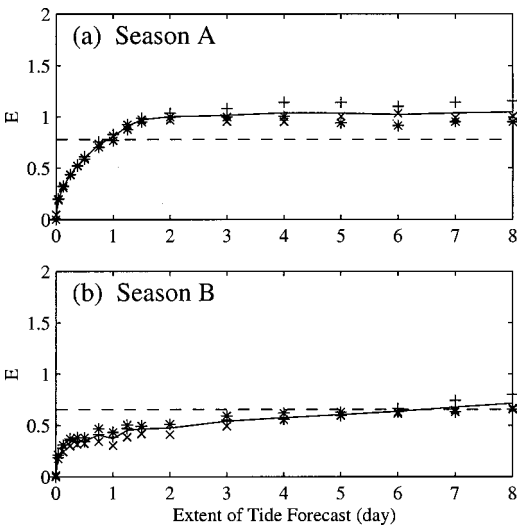

Fig. 3. Limitations of tide forecasts for Galveston for Season A (a) and Season B (b). Dashed horizontal line indicates normalized error E between observations and unadjusted tide prediction. Error of adjusted water level predictions is indicated for each year by discrete points ($\times=1999$; $+=1998$; $*=1997$) and average shown by solid line.

J. Waterway, Port, Coastal, Ocean Eng., 2002, 128(1): 21-29

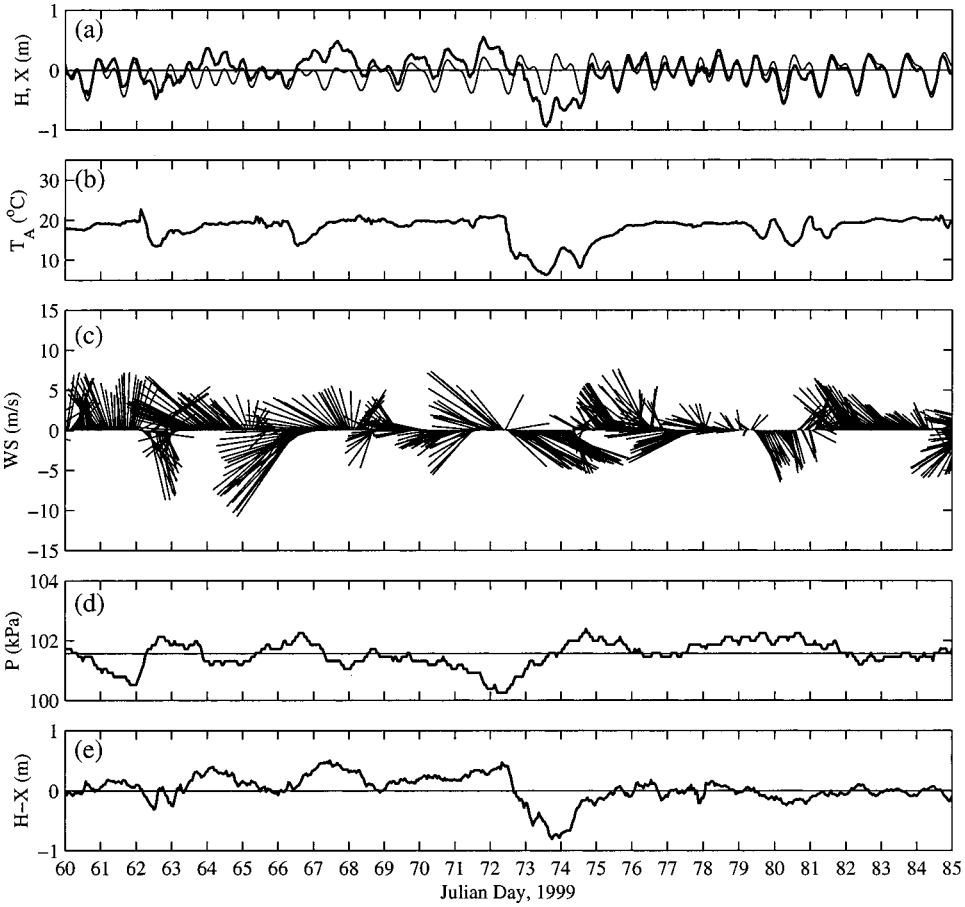

Fig. 4. Temporal variation of observations at Galveston Pleasure Pier for $60<Jd<85$, 1999, with (a) observed water level (heavy solid) and tide prediction (light); (b) air temperature; (c) wind speed and direction where line point in direction of flow; (d) barometric pressure; and (e) water level anomaly

relationship is not symmetric (compare columns 2 and 3). Nevertheless, the data suggest a simple linear model in which the anomaly is proportional to the square of the wind speed projected on the east-west axis, $(H-X)=c_1 v|v|$. The constant of proportionality c_1 is optimized by minimizing the least-square error for the existing data. In addition to c_1, the model can be optimized to account for the lag between the wind and the anomaly, since the change in the water level anomaly occurs several hours after the passage of the front. Optimization curves for lag between the wind and anomaly t_{lag} and the calibration coefficient c_1 are shown in Fig. 7 for 1999. The figure shows that the model is robust and not overly sensitive to the value of c_1 (i.e., the optimization curve is fairly flat for the range of values tested). Furthermore, the lag between the wind shift and water level anomaly is approximately $t_{\text{lag}}=9$ h for Season A for all three years.

Fig. 8 shows the model results for a portion of the record $65<Jd<85$ for 1999. Fig. 8(a) shows the observed water level and harmonic predictions, highlighting the fact that the harmonic predictions are not accurate during the passage of the fronts ($Jd\simeq 73$) but give reasonably good predictions when the wind forcing is low ($Jd\simeq 83$). Fig. 8(b) shows the observed water level anomaly and anomaly prediction using $(H-X)=c_1 v|v|$ with $c_1=-1/230\ \text{s}^2/\text{m}$ and $t_{\text{lag}}=9$ h. Fig. 8(c) shows water level observations with the harmonic plus anomaly predictions. Although the linear model is crude, it gives a reasonable first approximation to improve the water level predictions by accounting for the meteorological forcing. Fig. 8(c) also shows an improved model that is refined using a neural network approach, as discussed in the next section.

Since the linear model relies on the wind input and has a lag of 9 hours, it is limited to short-term forecasts of 9 hours or less. However, the model can be extended by using forecasted weather information (e.g., marine forecasts from the National Weather Service) as input. As a first approximation, the wind forecasts were simulated using the observed wind speeds, to which noise was added based on a Gaussian distribution to simulate the uncertainty of the forecasts. The forecasted wind speed, v_f, is obtained as $v_f=v+\Delta v$, where v east-west wind speed, and $\Delta v=f(v,\sigma_{v_f})$ was a random number based on a Gaussian distribution. The standard deviation for the distribution varied with the extent of the forecast as follows: $\sigma_{v_f}=0.5\sigma_v$ (+6 h), $1.0\sigma_v$ (+12 h), $1.5\sigma_v$ (+18 h), $2.0\sigma_v$ (+24 h), where σ_v standard deviation of the unsmoothed wind speed over the entire record. No attempt was made to vary the wind direction. Fig. 9 shows an example of the 24-hour simulated wind forecast as compared with the observed wind speed. A comparison of observations with the 12-hour marine forecasts from the National Weather Service is presented in the appendix.

Fig. 10 is a detail of Fig. 3 for Season A showing the improvements of the linear model over harmonic analysis in making short-term water level predictions. The abscissa is in hours and

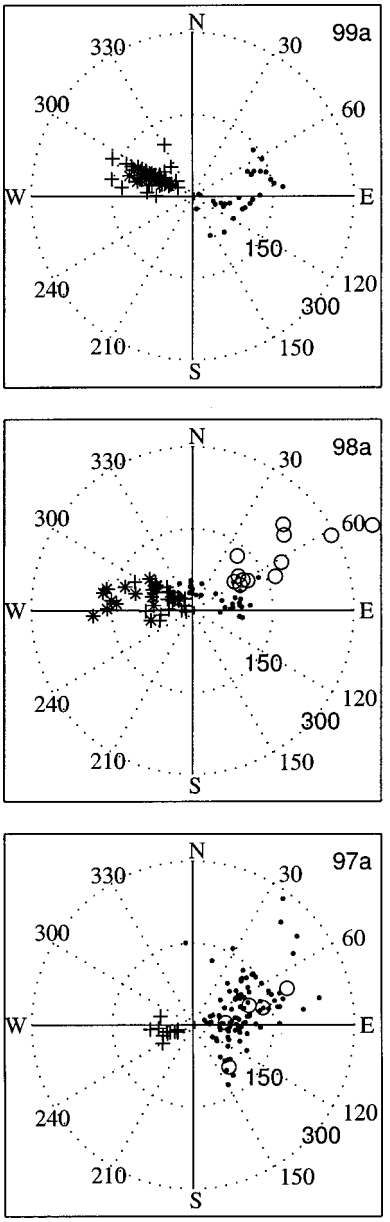

Fig. 5. Polar plot 1997–1999 of water level anomaly with $(H-X)<-3\sigma_X$ (×), $-3\sigma_X<(H-X)<-2\sigma_X$ (+), $2\sigma x<(H-X)<3\sigma_X$ (●), and $(H-X)>3\sigma_X$ (○) and $\sigma_X=0.198$, 0.195, 0.192 m for 1999a, 1998a, and 1997a. θ indicates direction from which wind is blowing. Radial distance indicates wind speed squared. Anomaly data are plotted to reflect 9 h lag between wind and water level response.

the ordinate is the error. The light horizontal line and the light solid line show the error for the unadjusted and adjusted water level predictions based on the harmonic analysis presented previously.

The heavy dashed line shows the error for the unadjusted linear model for Season A (average over three years). For $t<9$ h, the model predictions are based on the measured wind speed without the simulated forecasts. For short-term predictions, the linear model reduced the error in half. For $t>9$ h, the predictions are based on the simulated forecasts and the error increases as the uncertainty of the forecasts (modeled by the standard deviation) increases. The solid line shows the average error for the adjusted linear model predictions. For $t<9$ h, the error in the linear model prediction is approximately the same as that of the harmonic

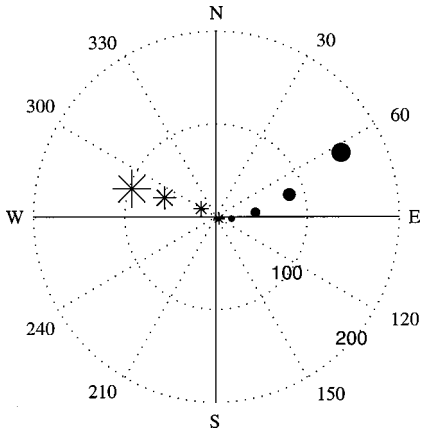

Fig. 6. Polar plot of mean anomaly for Season A, from 1997 to 1999. Solid circles indicate positive anomaly, asterisks indicate negative anomaly, and increasing symbol size indicates increasing strength of anomaly with values listed in Table 2. θ indicates direction from which wind is blowing. Radial distance indicates wind speed squared. Anomaly data are plotted to reflect 9 hour lag between wind and water level response.

model with an adjusted water level. However, for $t>9$ h, the adjusted linear model outperforms both the unadjusted linear model and the adjusted harmonic prediction. The dash-dot line indicates the performance of the neural network model discussed in the next section.

Neural Network Model

Although the linear model is robust and significantly reduces the error in the water level predictions, Figs. 4–6 and Table 2 show that the model is an oversimplification in that it only accounts for the wind projected on the east-west axis, is linear, requires a priori knowledge of the phase lag between wind and water level anomaly, and does not include barometric effects. To overcome these shortcomings, a neural network model is proposed that incorporates east-west and north-south directed wind speed, barometric pressure, and the water anomaly itself. Furthermore, it is less dependent on knowledge of the phase lag between wind and water level variation.

Neural networks have been recently applied to coastal engineering to predict monthly water levels (Vaziri 1997), hourly tides (Tsai and Lee 1999), coastal structure response (Mase et al. 1995; Van Gent and van den Booraard 1998), and runoff and drainage

Table 2. Summary of Anomaly Statistics for Season A Averaged over Three Years

Range	$\overline{H-X}$ (m)	$\overline{v\|v\|}$ (m^2/s^2)	$\overline{\theta}$ (°)
$HX/\sigma_X>3$	+0.67	153	63
$2<HX/\sigma_X\leq 3$	+0.45	84	74
$1<HX/\sigma_X\leq 2$	0.27	43	84
$0<HX/\sigma_X\leq 1$	+0.09	17	97
$-1<HX/\sigma_X\leq 0$	−0.08	4	124
$-2<HX/\sigma_X\leq -1$	−0.27	19	298
$-3<HX/\sigma_X\leq -2$	−0.46	60	290
$HX/\sigma_X<-3$	−0.69	97	288

J. Waterway, Port, Coastal, Ocean Eng., 2002, 128(1): 21-29

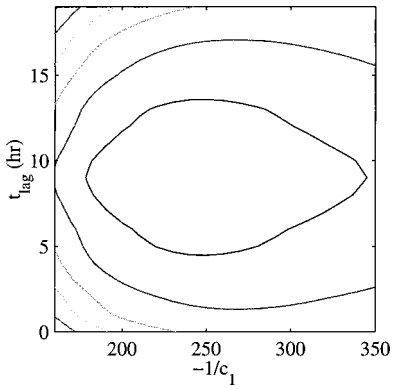

Fig. 7. Optimization curves for linear model for 1999. Contours indicate minimized error, E, with optimum lag $t_{lag}=9$ h and coefficient $c_1=-1/230\ s^2/m$ to give minimum error.

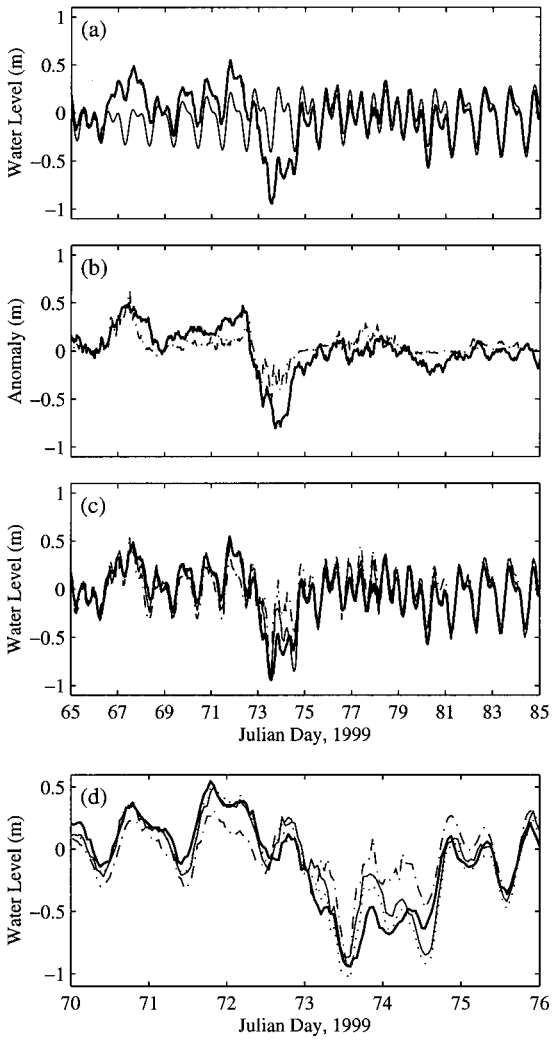

Fig. 8. Water level observations (heavy line) and harmonic predictions (a); water level anomaly (heavy) and 9-hour predictions based on $c_1 v|v|$ with $t_{lag}=9$ h and coefficient $c_1=-1/230\ s^2/m$ (dash-dot) (b); and observations (heavy), linear model prediction (dash-dot), and Neural Network Predictions (solid) (c) for $65<Jd<85$, 1999, and detail (d) for $70<Jd<76$ with observations (heavy), linear (dash-dot), NN model trained in 1997 (solid) and NN model trained in 1998 (dotted).

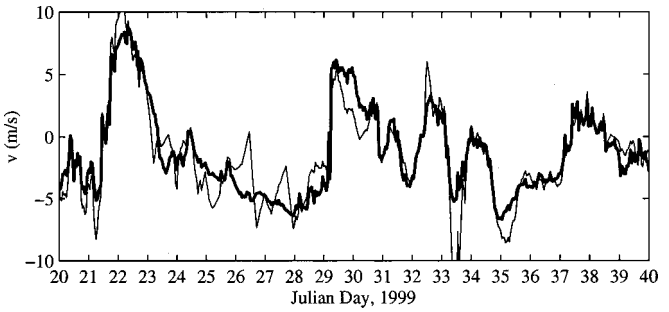

Fig. 9. Simulated 24-h forecast (light line) of wind speed using random number with Gaussian distribution with observed wind speed (heavy line).

(Campolo et al. 1997; Proano et al. 1998), as well as forecasting for natural phenomena (e.g., French et al. 1992; Recknagel et al. 1997; Corchado and Fyfe 1999). Whereas Tsai and Lee (1999) used neural networks for one-hour predictions of tidal variations in the absence of significant meteorological events [see also Kumar and Minocha (2001), Mandal (2001), Medina (2001), Walton and Garcia (2001), and Tsai and Lee (2001), for a discussion of that paper], the present model relies on harmonic analysis to predict the tidal fluctuations and neural networks to predict the anomaly.

The neural network model was trained using a back-propagation algorithm, and all computations were performed within the MATLAB 5.3/version 3 of the Neural Network Toolbox (Neural 1998). A simple neural network structure based on one hidden layer (H) and one output layer (O) was found to be optimal in forecasting the anomaly. Logsig and tansig transfer functions were used for the hidden and output layers, respectively, and the input decks were scaled to a $[-1,1]$ range. The optimal structure of the input deck depended on the extent of the forecast and the inclusion of forecasted winds.

For this work, an input deck (I) including time series of five previous hourly measurements of water anomalies, east-west wind speed squared, and north-south wind speed squared, and 20 hourly measurements of the barometric pressure complemented the forecasted wind. The final structure of the neural network was typically of the type I37H1O1. The inclusion of forecasted winds improved the model skill beyond six hours and was a dominant factor for extended forecasts. The neural network was trained over one data set (1997, 1998, or 1999) and evaluated over the two other data sets not included in the training.

Fig. 8(c) shows the performance of the neural network model compared with the simple linear model and the observed water level fluctuations. The neural network model results are 9 hour predictions based on the simulated wind forecast discussed previously and do not include the assumed 9 hour phase lag, as was the case for the simple linear model.

Fig. 8(d) shows the detail for the frontal passage for $70<Jd<76$. This panel shows the observed water level (heavy solid line), the simple linear model (dash-dot), and two predictions made by the neural network model. For the first neural network prediction, the model was trained using data from 1997 (light solid), and for the second prediction, it was trained using data from 1998 (dotted). Both predictions yield similar results, showing that the model is not sensitive to the training. Both predictions greatly improve on the simple linear model, particularly with the strong east winds preceding the front causing a large positive anomaly ($Jd\simeq 72$). The neural network model also improves the

J. Waterway, Port, Coastal, Ocean Eng., 2002, 128(1): 21-29

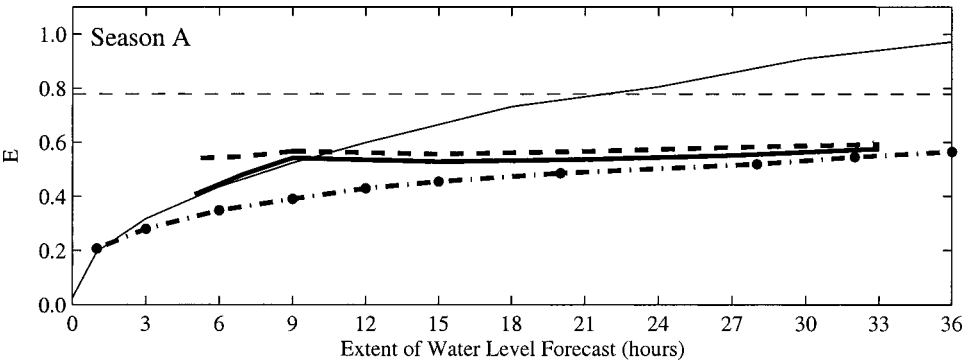

Fig. 10. Error estimates, E, between observed water level and predictions using unadjusted tide harmonics (light dashed), adjusted tide harmonics (light solid), mean error for unadjusted linear model (heavy dash), and adjusted linear model (heavy solid), and mean for NN model (dash-dot). Linear model predictions for $t>9$ h and NN model predictions for $t>0$ h are based on simulated wind forecasts.

prediction of the large negative anomaly ($73<Jd<74$) due to the west winds after the passage of the front.

Fig. 10 shows the overall improvement of the neural network model in reducing the error for Season A. The neural network model is used here to make up to 36 hour predictions of the water level anomaly, which is then added to the tide (harmonic) prediction to predict the total water level variation. As a first attempt to show the utility of the refined neural network model, anomaly forecasts are based on the simulated wind forecasts, as described previously. Up to 18 hour forecasts, simulated and exact wind forecasts yield the same results within two standard deviations. For forecast times larger than 18 hours, the skill of the model based on exact winds increasingly outperforms the simulated wind case, as expected. The use of the actual marine forecasts will be addressed in future work. Nevertheless, Fig. 10 clearly shows the utility of making short term ($3<t<24$ h) water level forecasts including the meteorological forcing by means of a neural network model. Further improvements to the model could include longer training sets with a larger number of frontal passages or the use of a hybrid model approach with one model trained on the complete data set and one model trained for frontal passages only.

Summary

The entrance to Galveston Bay plays a critical economic role in commercial shipping. It is therefore crucial to have accurate short term water level predictions for the safe navigation of deep draft vessels. The wind plays a crucial role in determining the total water level in the region because of the shallow conditions along the northern Gulf of Mexico coast and low tidal oscillations. Although there have been many recent advances such as real-time access to wind and water level information for this area, the present state-of-the-practice is to rely on water level predictions based on harmonic analysis (e.g., tide tables), which can not include short-term meterological events such as cold fronts.

The following conclusions are drawn from observed wind and water levels at one location near the entrance of Galveston Bay during two distinct seasons over three years:

1. For extremely short-term water level predictions ($0<t<3$ h), harmonic analysis yields accurate predictions, provided that they are adjusted using the known water level anomaly at the present time. This ''adjusted method'' works better in the summer months, since the difference between the observed water level and that predicted by harmonic

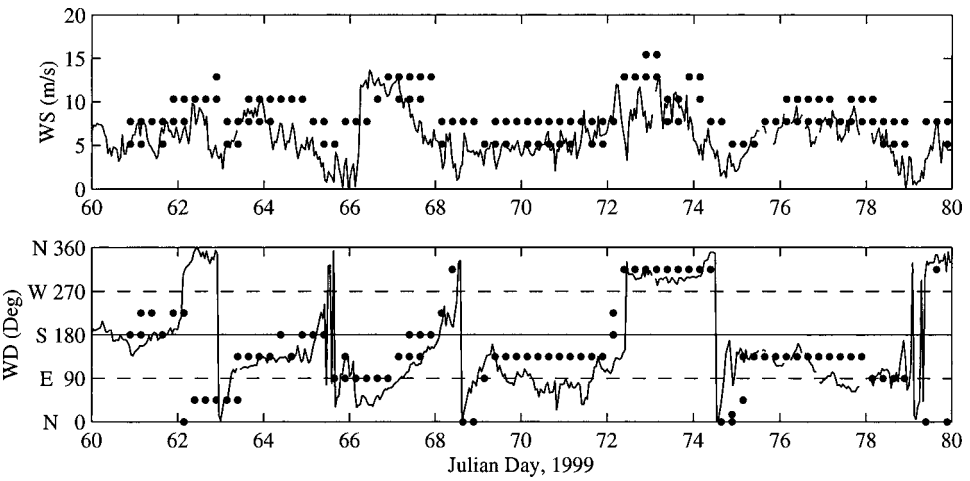

Fig. 11. Comparison of 12-h coastal marine forecast of wind speed and direction from the National Weather Service (solid dots) with observations (light line) for $60<Jd<80$, 1999

J. Waterway, Port, Coastal, Ocean Eng., 2002, 128(1): 21-29

analysis is generally due to phenomena that act on longer time scales. The accuracy of this ''adjusted method'' decreases as the extent of the forecast increases, particularly in the spring months, because the water level responds in a matter of hours to the passage of cold fronts. For $t>24$ h, the adjusted method is worse than conventional harmonic analysis.

2. The water level anomaly in the spring months is primarily due to the east-west component of the wind stress and the water level anomaly can be as large as the tidal motion itself.
3. The water level anomaly can be reasonably well predicted up to 9 h using the local observed wind speed squared projected onto the east-west axis. The simple model has one calibration coefficient, which is robust and does not need to be adjusted.
4. The model can predict the water level anomaly for $t>9$ h to the extent that the meteorological conditions can be predicted. Based on simulated wind forecasts using the observed winds and noise added with a Gaussian distribution, the linear model outperforms the predictions based on conventional harmonic analysis and the adjusted model.
5. The linear model is further refined using a neural network approach that includes barometric pressure and the orthogonal wind component. The neural network model significantly outperforms the adjusted harmonic model for short term forecasts ($3<t<9$ h) and the linear model for longer forecasts ($9<t<24$ h).
6. For $t>24$ h, both the linear model and the neural network model outperform the predictions based on harmonic analysis. For this extent of forecast, the neural network model is almost completely dependent on the forecast data.

Although the forecasted winds were simulated based on the observed winds with noise added, comparisons of the observed winds with the National Weather Service forecasts (Appendix) show that it is likely the National Weather Service marine forecasts are of sufficient accuracy to aid in the short term (e.g., 24 h) prediction of the water level anomaly and can be used to aid in navigation, oil spill response, and search and rescue in the entrance of Galveston Bay. This paper shows the potential modeling approach using neural networks and extension of this work to include the predictions of channel currents and the prediction of the water level at other locations along the coast is ongoing. The physical mechanisms to explain the success of the east-west wind stress component in predicting the water level anomaly is also needed, and Fig. 6 indicates that the simple projection of the wind stress onto the east-west axis may be an oversimplification. Additional research is needed to show the potential use of neural network modeling for prediction of the water levels and meteorological events for coastal regions. A complete comparison of the linear and neural networking approaches must be made in a consistent manner. This topic will be addressed later in a companion paper.

Acknowledgments

The writers thank John Metz of the National Weather Service for providing the historical records of the coastal marine forecasts. Joel Darnell prepared these records for comparison with the observed wind data. The writers acknowledge and thank the Texas General Land Office, the Texas Water Development Board, the U.S. Army Corps of Engineers Galveston District, and the National Ocean Service for their ongoing support for the TCOON network and for providing the data used in this study. The writers thank the two anonymous reviewers for their comments. This research was supported by the National Science Foundation award CTS-9734109.

Appendix: Comparison with National Weather Service Forecasts

Although it is beyond the scope of this paper to compare the accuracy of the marine forecasts from the National Weather Service, it is instructive to see the qualitative accuracy of these forecasts and whether they would be suitable as input to a water level forecasting model. Fig. 11 compares the 12-hour National Weather Service forecasted wind speed and direction for the coastal waters near Galveston from $60<Jd<80$, 1999. The reports are generally issued four times per day in a text format, often with a range of wind speed and directions. The text-based data were converted to numerical values, and two data points at the same time indicate when a range was given. The comparisons indicate that, although the wind speeds are generally overpredicted, the passage of frontal systems (e.g., $71<Jd<73$) are generally well predicted. Therefore, it is feasible to construct a neural network model for short term water level predictions at the entrance to Galveston Bay derived from locally forecasted wind speed and direction.

References

Campolo, M., Andreussi, P., and Soldati, A. (1997). ''River flood forecasting with a neural network model.'' *Water Resour. Res.*, 35(4), 1191–1197.

Cochrane, J. D., and Kelly, F. J. (1986). ''Low-frequency circulation on the Texas-Louisiana continental shelf.'' *J. Geophys. Res.*, 91(c9), 10645–10659.

Corchado, J. M., and Fyfe, C. (1999). ''Unsupervised neural method for temperature forecasting.'' *Artif. Intell. Eng.*, 13, 351–357.

French, M. N., Krajeski, W. F., and Cuykendall, R. R. (1992). ''Rainfall forecasting in space and time using a neural network.'' *J. Hydrol.*, 137, 1–31.

Kumar, A., and Minocha, V. K. (2001). ''Discussion of 'Back-propagating neural network in tidal-level forecasting,' by Ching-Piao Tsai and Tson-Ling Lee.'' *J. Waterw., Port, Coastal, Ocean Eng.*, 127(1), 54–55.

Mandal, S. (2001). ''Discussion of 'Back-propagating neural network in tidal-level forecasting,' by Ching-Piao Tsai and Tson-Ling Lee.'' *J. Waterw., Port, Coastal, Ocean Eng.*, 127(1), 55.

Mase, H., Sakamoto, M., and Sakai, T. (1995). ''Neural network for stability analysis of rubble-mound breakwaters.'' *J. Waterw., Port, Coastal, Ocean Eng.*, 121(6), 294–299.

Medina, J. R. (2001). ''Discussion of 'Back-propagating neural network in tidal-level forecasting,' by Ching-Piao Tsai and Tson-Ling Lee.'' *J. Waterw., Port, Coastal, Ocean Eng.*, 127(1), 55–57.

Michaud, P. R., Thurlow, C. I., and Jeffress, G. A. (1994). ''Collection and dissemination of marine information from the Texas Coastal Ocean Observation Network.'' *Proc., U.S. Hydr. Conf.*, Hydrography Society, Norfolk, Va., 168–173.

Neural Network Toolbox for use with Matlab 5.3/version 3. (1998). The MathWorks, Natick, Mass.

National Oceanic and Atmospheric Administration (NOAA). (1994). ''Special 1994 tidal current predictions for Aransas Pass, Corpus Christi, Texas.'' *NOAA Technical Memorandum NOS OES 8*, U.S. Department of Commerce, Washington, D.C.

National Oceanic and Atmospheric Administration (NOAA). (1999). ''Assessment of the National Ocean Service's tidal current program.''*NOAA Technical Rep. NOS Co-OPS 022*, U.S. Department of Commerce, Washington, D.C.

Proano, C. O., Minn, A. W., Verwey, A., and van den Boogaard, H. F. P. (1998). ''Emulation of a sewerage system computational model for the statistical processing of large numbers of simulations.'' *Hydroinformatics '98*, Balkema, Rotterdam, The Netherlands, 1145–1152.

Recknagel, F., French, M., Harkonen, P., and Yabunaka, K.-I. (1997). ''Artificial neural network approach for modelling and prediction of algal blooms.'' *Ecological Modelling*, 96, 11–28.

Smith, N. P. (1978). ''Long-period, estuarine-shelf exchanges in response to meteorological forcing.'' *Hydrodynamics of estuaries and fjords*, J. C. J. Nichoul, ed., Elsevier, New York, 147–159.

Tsai, C.-P., and Lee, T.-L. (1999). ''Back-propagation neural network in tidal-level forecasting.'' *J. Waterw., Port, Coastal, Ocean Eng.*, 125(4), 195–202.

Tsai, C.-P., and Lee, T.-L. (2001). ''Closure to 'Back-propagating neural network in tidal-level forecasting.' '' *J. Waterw., Port, Coastal, Ocean Eng.*, 127(1), 58–59.

Van Gent, M. R. A., and van den Booraard, H. F. P. (1998). ''Neural network modeling of forces on vertical structures.'' *Proc., Int. Conf. on Coastal Engineering*, B. L. Edge, ed., ASCE, Reston, Va., 2, 2096–2109.

Vaziri, M. (1997). ''Predicting Caspian Sea surface water level by ANN and ARIMA models.'' *J. Waterw., Port, Coastal, Ocean Eng.*, 123(4), 158–162.

Walton, T., and Garcia, A. W. (2001). ''Discussion of 'Back-propagating neural network in tidal-level forecasting,' by Ching-Piao Tsai and Tsong-Lin Lee.'' *J. Waterw., Port, Coastal, Ocean Eng.*, 127(1), 57–58.

Whitaker, R. E. (1971). ''Seasonal variations of steric and recorded sea level of the Gulf of Mexico.'' MS thesis, Dept. of Oceanography, Texas A&M Univ., College Station, Tex.

Wu, J. (1980). ''Wind stress coefficients over sea surface near neutral conditions—a revisit.'' *J. Phys. Oceanogr.*, 10, 727–740.

J. Waterway, Port, Coastal, Ocean Eng., 2002, 128(1): 21-29